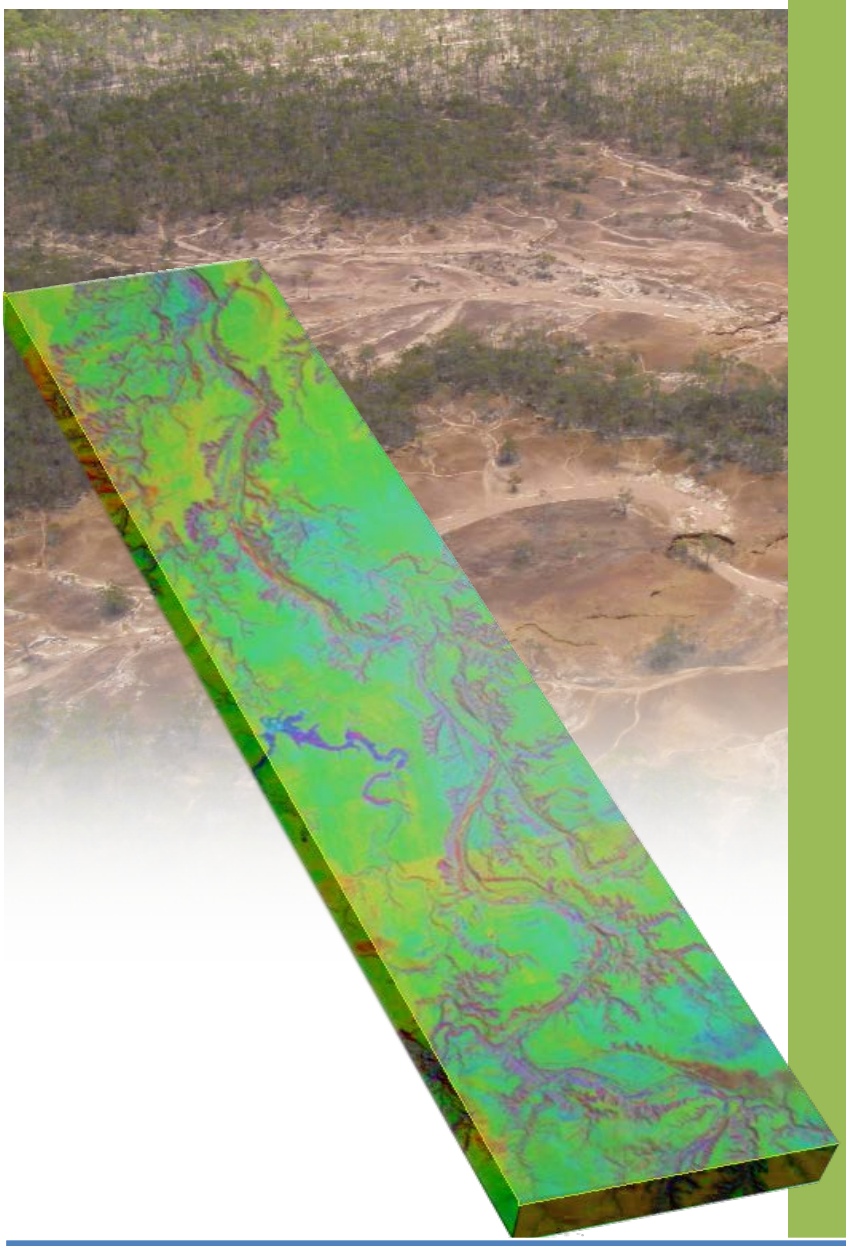

An Empirically-based Sediment Budget for the Normanby Basin

Andrew Brooks, John Spencer, Jon Olley, Tim Pietsch, Daniel Borombovits, Graeme Curwen, Jeff Shellberg, Christina Howley, Angela Gleeson, Andrew Simon, Natasha Bankhead, Danny Klimetz, Leila Eslami-Endargoli, Anne Bourgeault

Australian Rivers Institute

Griffith University

Appendix 10: Age, distribution and significance within a sediment budget of in-channel benches in the Normanby River

Griffith UNIVERSITY

CARING FOR OUR COUNTRY

Appendix to the Final Report prepared for the Australian Government's Caring for our Country - **Reef Rescue initiative**

IMPORTANT

This document is current at the date noted. Due to the nature of collaborative academic publishing, this content is subject to change and revision. Please see the Cape York Water Quality website for more info:
http://www.capeyorkwaterquality.info

This Version: 3/03/2013

CAPE YORK WATER QUALITY

Appendix 10: Age, distribution and significance within a sediment budget of in-channel benches in the Normanby River

Prepared by: Pietsch*, T.J., Brooks, A.P., Spencer, J., Olley, J.M., Borombovits, D.

Australian Rivers Institute, Griffith University, Nathan, QLD 4111, Australia

***Corresponding author:** t.pietsch@griffith.edu.au

Abstract

Here we present the results of investigations into alluvial deposition in the catchment of the Normanby River, which flows into Princess Charlotte Bay (PCB). Our focus is on the fine fraction (<~63 um) of alluvial deposits that sit above the sand and gravel bars of the channel floor, but below the expansive flat surface generally referred to as the floodplain. Variously described as benches, bank attached bars or inset or inner floodplains, these more or less flat-lying surfaces within the macro channel have hitherto received little attention in sediment budgeting models. Here we use high resolution LiDAR based mapping combined with optical dating of exposures cut into these in-channel deposits to compare their aggradation rates with those found in other depositional zones in the catchment, namely the floodplain and coastal plain. In total 53 single grain OSL dates were produced across 20 stratigraphic profiles at 15 sites distributed though the 27 600km^2 catchment. We show that in-channel storage is a significant component of the fine sediment budget, representing more than 15% of the volume entering the channel network from hillslopes and subsoil sources and therefore, at the very least, in-channel storage of fine material needs to be incorporated into sediment budgeting exercises.

1. Introduction

The Normanby catchment, including the conjoined catchments of the Stewart, Hann, North Kennedy, Annie and Morehead Rivers, covers an area of approximately 27 600 km^2 in tropical north Queensland, Australia (Fig. 1). Mean annual run-off between 1986 – 2009 is estimated at 4,600 GL/year. The climate is characterised by extreme rainy (summer) and dry (winter) seasons with 95% of its annual rainfall occurring between the months of November and April. Consisting of predominantly low relief plains in the north and undulating rises and dissected plateaus in the south, the Normanby drains into Princess

Charlotte Bay (PCB) which in turn opens onto the Great Barrier Reef (GBR) lagoon. Despite retaining much of its 'natural' vegetation cover, and being very sparsely populated (< 500 permanent residents) the catchment has been identified as one of the most significant contributors of suspended sediment to the GBR (Prosser et al., 2001, Brodie et al., 2003), though this assertion is now being challenged (Fabricious et al. 2005) along with the assumption that underlie it (Brooks et al, 2012). Much of the earlier conclusions as to the significance of the Normanby as a source for sediment to the GBR arose out of sediment budget exercises, whereby sources and sinks of sediment throughout the catchment are organised into a modelled framework acquitting one against the other. The sediment budget concept has been a central organising principle within the discipline of geomorphology since at least the 1970s (Dietrich and Dunne, 1978; Dunne and Leopold, 1978), with the concept increasingly refined in subsequent decades. In essence a sediment budget provides a method of accounting for sediment inputs and outputs through a drainage network. It enables the primary source of sediment and the sediment transport pathways to be identified, and is useful for highlighting data needs and system understanding (or lack thereof). This paper accompanies a group of companion papers (Brooks et al; Olley et al; Spencer et al) that arise out of an Australian Government funded project that sought to parameterise with newly collected empirical data a (spatially and temporally) higher resolution catchment model for the Normanby. In this paper we focus on the distribution and rates of aggradation of in-channel deposits, but we also include comparable investigations into the floodplain and the broad coastal plain at the very bottom of the catchment. These data allow the rates of deposition and storage of fine sediment within the channel to be placed in a broader context.

Fig.1 Map of the Normanby catchment showing major channels and location of LiDAR blocks and sampling sites.

Alluvial deposits that sit within the channel boundary but are too high to be considered part of the mobile bed have recently been the subject of renewed research effort in Australia, especially in relation to their role within sediment transport pathways (e.g. Rustomji and Pietsch, 2007; Hughes et al, 2009; Wasson et al, 2010). There is a growing realisation that understanding the dynamics of these deposits is crucial to understanding the transport of sediments from and through catchments. The perceived importance of these deposits may, in part, be due to the highly episodic nature of flow in many Australian catchments (Finlayson and McMahon, 1988; Kemp, 2004; Rustomji et al., 2009). Flow over the high floodplain is a rare occurrence and deposition thereon a consequently insignificant part of the sediment budget in most years. Our observations of large expanses of depositional zones (which henceforth we refer to collectively as in-channel benches) within the channels of the Normanby lead us to hypothesise that they may be a more significant sediment store than the high alluvial surface traditionally termed the floodplain, or at least significant enough that excluding them from a catchment sediment budget would result in it being significantly in error. This study seeks to test this hypothesis.

2. Methods

2.1 Site Selection

Five bench sites distributed throughout the catchment, judged to be broadly representative of the styles of in-channel bench found within the Normanby catchment, were selected for stratigraphic investigation and assessment of aggradation rate. An additional site (East Normanby) was selected for intensive investigation of the variation in aggradation rate within a channel; whereby multiple aggradation rates for different surfaces with different elevations above the thalweg were determined. A further seven floodplain sites, generally exposures in stream banks, were selected for determination of aggradation rate on the high floodplain. Finally, two sites on the broad coastal plain at the lowermost part of the catchment were included for investigation. Sampling locations are shown in Figure 1.

Fig 1 Normanby Catchment showing location of LiDAR blocks, bench, floodplain and coastal plain sites.

2.2 Field Stratigraphy

At each sampling location pits were hand dug or fresh faces were cut in existing exposures. The coastal plain section was supplemented by hand augering to depth. Stratigraphic descriptions were made in the field, supplemented by investigation of sediments under a binocular microscope and particle size analysis.

2.3 Bench mapping using LiDAR

Light Detection and Ranging data (LiDAR) of 35 blocks (Fig. 1) of the catchment covering and area of xkm^2 (XX% of the catchment) was flown in between May and August 2009 by *Terranean* (now RPS) as part of a larger study of the catchments (Brooks et al., submitted). Flight lines were designed to achieve a point density of 2.3 points per square metre and 43% overlap over the project areas. The flying height was (nominally) 600 metres above ground level. The LiDAR points were classified as ground and non-ground points using automatic filtering followed by interactive checking and re-classification. The automatic classification was performed using TerraScan software. Once the point clouds had been formed and classified. Raster surfaces were generated from the LiDAR LAS files. The ground pixel spacing of the rasters is one metre. The rasters were provided to the authors by *Terranean* in ESRI ASCI grid format. An automated approach to bench delineation using this data within ARC GIS was adopted. Firstly, we derived a 'flat area' layer for each of 35 LiDAR blocks) by selecting those areas with less than 8^o slope, presuming these to be the zones of maximum deposition (Fig. 2). Where LiDAR blocks covered junctions of major channels, the channel was divided into three reaches (below junction; left tributary; right tributary) for further analysis. To reduce processing times, this layer was clipped using a hand digitised polygon that incorporated all of the channel and enough of the upper floodplain to ensure no component of the channel was excluded via operator bias as regarding what constitutes the channel edge. An elevation above thalweg was then determined for each 1 m grid cell comprising the 'flat area' using the 'Spatial Join' function within ARC GIS. Each grid cell was

compared in elevation to the nearest part of the channel thalweg, with the thalweg digitised by hand. In many places the true thalweg could not be identified due to the presence of standing water, in these cases the thalweg was simply mapped as the centreline of the waterbody. Though this introduces a small inaccuracy, it is not considered significant as, in most cases, the depth of standing water during the dry season (when the LiDAR data was collected) is shallow (<0.5 m) in comparison to the overall relief of the channel bed (>2m).

Fig. 2 Processing steps used to delineate benches using high resolution LiDAR data. Extract from LiDAR block 5 shown.

The distribution of the 'flat area' elevations relative to the thalweg was then described by summarising all elevations for each LiDAR block within a frequency histogram (Fig. 3). Presented in this way, the height of the floodplain is clearly marked by a peak in the frequency histogram centred on the average depth of the macro channel. The other reoccurring feature of these plots is a peak centred on zero, with the positive spread in this peak representing the bed relief and unavoidable artefacts of the TIN derived water surface. In some, but not all, such plots distinct concentrations between the thalweg and floodplain peaks occur, with these appearing as discrete benches in the field. Where no within channel depositional areas exist, a characteristic u-shaped distribution occurs; whereas large areas of gently sloping surface or large numbers of benches with closely spaced elevations, result in a continuum between thalweg and floodplain with no particular peaks observable.

Fig.3 Frequency histogram for elevations above the thalweg for LiDAR block 5.

The flat-area-height above thalweg histograms allow description of the distribution of within channel surfaces; calculation of the total area of within channel depositional area via observation of the area below each curve, and finally, the area of any individual surface (or combination of surfaces) with a single height above the thalweg via distribution deconvolution. This has been facilitated by fitting normal (Gaussian) distributions to peaks representing discrete benches. Though the choice of this distribution shape is somewhat arbitrary, it accords with our observations of a roughly sigmoidal cross sectional form of most bench surfaces.

2.4 Particle Size Analysis

All samples collected for OSL analysis had sub-samples collected for particle size analysis, undertaken using a Malvern Mastersizer 2000, using protocols developed by the Queensland Dept. Natural Resources and Mines. Samples were mechanically agitated and ultrasonically dispersed before and during measurement.

2.5 Optical Dating

In total 53 samples were collected for optical dating by driving stainless steel tubes into cleaned exposures or the base of boreholes. Sample preparation was designed to isolate pure extracts of 180-212 µm light safe quartz grains, collected from the centre of the cores, following standard procedures (e.g. Aitken, 1998) under subdued red light. Treatments were applied to remove contaminant clays, carbonates, feldspars, organics,

heavy minerals and acid soluble fluorides. The outer ~10 µm alpha-irradiated rind of each grain was removed by double etching each sample in 48% hydrofluoric acid.

Single-grain equivalent dose (De) values were determined using the modified single aliquot-regenerative dose (SAR) protocol of Olley et al (2004) and Risø instrumentation described therein, in combination with the acceptance / rejection criteria provided in Pietsch (2009). An additional test based on examination of variations in the response to the test dose was also incorporated. Grains were rejected if either of the second or third Test Dose signals varied in sensitivity from the first Test Dose (associated with the Natural Dose) by more than 20%.

The age modelling approach of Galbraith and co-workers (Galbraith and Laslett, 1993; Galbraith et al., 1999; Roberts et al., 2000) was used to determine a burial dose from the population of single grain De values. First the central age model (CAM) was used to determine the overdispersion (σ_d) for each sample, with σd representing the degree of spread in the data beyond that which can be explained by known sources of uncertainty (i.e. measurement uncertainty on each individual single grain D_e). Non-zero σ_d values are almost universally found for single grain dose distributions. The greatest component of this is traditionally attributed to partial bleaching (e.g. Olley et al, 2004) however there are other important contributors, most notably β-dose heterogeneity (Nathan et al, 2003), but also variations in instrument uncertainty which has been shown to be sample dependent (Jacobs et al, 2006; Pietsch, 2009). Once the σ_d for each single grain dose population has been defined using the CAM, the minimum age model (MAM) is applied to identify the component of the dose distribution which represents those grains fully bleached at deposition. To do so requires adding in quadrature to each single grain D_e error, the absolute percentage of σ_d considered to originate from sources other than partial bleaching. In other words, it is necessary to determine how overdispersed the single grain D_e population would be, even if it was completely bleached at burial, prior to application of the MAM. Here we have determined the σ_d likely to exist within well bleached populations by identifying the lower limit of σ_d across all samples, with our assumptions being that at least some of our samples will be fully bleached, but that all samples will have the same degree of σ_d caused by other factors. Some proportion of our samples are likely to be well bleached and these should all have a consistent σd value, with this being a function of measurement conditions and the level of heterogeneity in the dose field within bench and floodplain deposits of the Normanby. Examination of the distribution of σ_d from all samples lead to the use of an applied σ_d of 20%, prior to application of the MAM and FMM.

Lithogenic radionuclide activity concentrations were determined using high-resolution gamma spectrometry (Murray et al. 1987), with dose rates calculated using the conversion factors of Stokes et al. (2003). β-attenuation factors were taken from Mejdahl (1979). Cosmic dose rates were calculated from Prescott and Hutton (1994) and long term water contents were estimated from observation of the range of measured water contents and consideration of the sampling location relative to the water table. Concentrations of ^{238}U, ^{226}Ra and ^{210}Pb are consistent with secular equilibrium in most samples. The minor secular disequilibrium observed in some samples is not sufficient to result in the calculation of an

age significantly different from that which would result from assuming equilibrium conditions to have persisted throughout the burial period. Hence, for simplicity, the ages have all been calculated using the as-measured radionuclide contents.

3. Results

3.1 In-channel bench delineation and distribution forms

Large alluvial surfaces below the upper floodplain have been found to be widespread, occurring to some extent in virtually all reaches of major channel in the Normanby Catchment. Fig. 3b illustrates a typical example, showing within channel benches extending on both sides of the low channel, and occupying, in this case, more than 100 m^2 for each linear metre of channel thalweg. Table 1 summarises the distribution throughout the major channel network of within channel benches, with an average of 180 m^2 of bench surface per linear meter of channel. Fig 4 illustrates the variety of distribution forms displayed through the catchment. Multimodality is clearest in the channels of the middle reaches of the catchment (e.g. Blocks 5,10,12 & 13), whilst lower reaches (Blocks 2, 25, 32) see more subdued, unimodal distributions indicating a single low bench between the water surface and the floodplain.

Fig. 4 Height above thalweg distributions for all LiDAR blocks. Arrow labelled 'fp' indicates floodplain in each case, whilst arrows labelled 'b' indicate benches.

3.2 Stratigraphy, age and aggradation rate

Bench stratigraphy varied from almost massive fine to medium sands (KPWN5), to well delineated sequences of ~decimetre thick units of sand and mud interpreted as being flood couplets (West Normanby; Battle Camp Crossing; Kalpowar; Carrols Crossing). The West Normanby Bench has accumulated sediment over the last 60 years (See Table 2 for full list of OSL dates) as a series of discrete units of sand and mud at an average rate of 31 mm/yr (Fig. 5). At Battle Camp Crossing, the couplet structure is more diffuse, but still recognisable (Fig. 6). There are two possible interpretations of the age depth profile for Battle Camp Crossing. For ~50 years prior to ~AD 1900 the bench accreted at a rate of 31 mm/a. Extrapolating this trend to the surface would indicate deposition at this site ceased approximately 70 years ago. However, the available alternative explanation is considered more likely, based on inspection of the stratigraphy, which does not show any obvious evidence of hiatus. That is, there has been a decline in aggradation rate since ~AD 1900, in accordance with what might be expected with increasing elevation above the thalweg, which results in an average aggradation rate since ~AD 1900 of ~10 mm/a. The bench at KPWN provided two ages which indicate a consistent aggradation rate of 2.3 mm/a for the last ~650years (Fig. 7), whilst the Kalpowar Bench has been accumulating over the last 200 years at approximately 13 mm/a, possibly slightly slower over the last ~60 years (Fig. 8). The higher surface at Kalpowar, some 1.5 metres above the bench has accumulated > 2m

over the last three thousand years, with the aggradation rate accelerating from ~0.4 mm/a between 3000 and 1000 years ago to ~1mm averaged over the last 1000 years.

Table 2. OSL data for each sample.

Fig. 5 a) Stratigraphy, b) OSL ages and aggradation model, and c) topography showing sampling location for the West Normanby Bench.

Fig. 6 a) Stratigraphy, b) OSL ages and aggradation model for the Battle Camp Crossing Bench. No cross-sectional or LiDAR data was collected for this site.

Fig. 7 Stratigraphy, OSL ages and aggradation model for the KPWN Bench

Fig.8 Stratigraphy, OSL ages and aggradation model for the Kalpowar Bench

The bench at Carols Crossing near Laura on the Laura River is very similar to the west Normanby bench, having multiple decimetre thick units of predominantly sand that have accumulated rapidly (~23 mm/a) over the last ~60 years. The Bench at Carols Crossing has apparently also seen three discreet units laid down in the last five or so years. These very young units are excluded from the aggradation calculation at this location.

Fig.9 a) Stratigraphy, OSL ages, b) aggradation model, c) topography and photo for the Carrols Crossing Bench

3.3 The relationship between height above thalweg and aggradation rate

The East Normanby site provides an opportunity to observe the effect of declining inundation frequency on aggradation rate (Fig. 10). A stepped scroll bar array forms a series of surfaces at different heights relative to the channel thalweg, each with its own inundation frequency. The lowermost unit consists of a ~2m thick sand bar attached to the inside bend, that has accumulated in the last few years, possibly even in the last year, given the complete lack of vegetation either at the surface or throughout the profile. A large sandy, vegetated scroll bar, running more or less concentric with the channel line, exists 3m higher up the bank and ~35m distal to the as surveyed waterline. This unit has been accreting over the last three hundred years, probably as a series of sand units equivalent in thickness and rapidity of deposition to the sand bar observed closer to the waterline. Below 1 m depth (and near 300 years ago) 180cm accumulated within the 100 years encompassed by the uncertainty bounds on the OSL ages., giving a minimum average accumulation rate of 18mm/a. The uppermost 60cm has accumulated at a rate between 4.2 and 10 mm/a. At a further 40m distal to the channel, is an older, higher scroll bar, similarly made of fine sand. Between ~1.8 and ~1.1 ka, this unit accumulated sediment at a rate of approximately 1.3mm/a, with the uppermost 70 cm accumulating at an average rate of 0.7mm/a. On the uppermost scroll bar observed at East Normanby, an augur hole revealed 2 m of fine sand, accumulating since 5.5 ka at an average rate of 0.4 mm/a.

Fig. 10 Topography, stratigraphy and age structure of scroll array at East Normanby. Age model plots omitted for clarity. d) shows relationship between aggradation rate and height above thalweg.

3.4 Floodplain Aggradation

Stratigraphy and age structure for all floodplain sites is summarised in Fig. 11. Bizant Gully shows evidence of a dramatic decline in aggradation rate. About 3500 years ago, approximately 1m of accretion occurred, at a rate sufficiently rapid that it occurred within the period bracketed by the uncertainty bounds on the dates (~700 yrs). This implies that the minimum aggradation rate during this period was ~1.4 mm/a. Extending this rate to the surface indicates that aggradation at this site ceased ~2500 years ago. Some incipient soil development at this location is consistent with this interpretation, though a very low aggradation rate (averaging 0.3 mm/a) cannot be excluded altogether. An aggradation rate of 0.8mm/yr is observable since ~2200 years ago at Bizant River. The age structure at IBA 16, though somewhat uncertain due to the multimodal nature of the single grain DE distribution at depth 50cm, clearly indicates an extremely low deposition rate. Of all the modes displayed in the distribution, it is not clear which, if any, represent the actual deposition age for that depth. It is likely that pedoturbation processes have resulted in the downward admixture of younger deposits, with this likely to have occurred during surface stability. The reported age for 50cm depth (2.53 ± 0.31 ka) should therefore be considered a minimum age, and the associated aggradation rate (~0.2 mm/a) a maximum.

Fig. 11 Stratigraphy and age structure for the floodplain sites.

There are three phases of aggradation observable at NSVF1. At about 3000 years ago almost a metre of sandy material accumulated within the time encompassed by the uncertainty bounds of the two bracketing ages, giving a minimum aggradation rate of 0.6mm/a. In the 2000 years following this another ~1m of slightly finer material accumulated at a rate of ~0.3mm/a. The uppermost 50cm of fine silty sand accumulated sometime in the last 1000yrs, at a rate of 0.5mm/a. Between ~10ka and ~4.8ka the floodplain beside the Morehead river accumulated sediment at 0.09 mm/a, with this approximately doubling since then to 0.2 mm/a. In contrast to the very slow aggradation rates observed for other proximal floodplain sites, the uppermost 180 cm of the floodplain beside the Normanby River aggraded comparatively rapidly around 600 years ago, that is, about 1 m within the 240 yrs encompassed by the combined uncertainty bands, or ~4.2 mm/a. Extrapolating this to the obvious stratigraphic break at 10cm indicates it likely formed after 400 yrs ago, giving a minimum aggradation rate of 0.25 mm/a. The uppermost ~10cm may overlap with European settlement. However, even it was deposited entirely within this period, than its deposition rate (~1 mm/a) would still be a quarter of that occurring in the previous 500 years.

3.5 Coastal Floodplains

At NKCP1, the uppermost two samples provide ages which overlap within uncertainties. In consideration of the uncertainties on the ages, the minimum aggradation rate between these two sample depths is 2.4 mm/a. Extending this to the surface suggests deposition ceased ~500 years ago. Sometime after this, the unit began to be eroded as evidenced by

the extensive scarp into which the exposure was cut, probably by a process of parallel retreat under the influence of wave action.

At NKCP2, the uppermost two samples likewise overlap within uncertainties, giving a minimum aggradation rate of 2.1 mm/a. Extending this to the surface suggests deposition ceased ~570 years ago. Although these sites are closely located (some 4km apart), the consistency in both the aggradation rates and estimated time of abandonment of the surface nonetheless supports their veracity.

Fig 12 Stratigraphy for two sites from pedestals within coastal plain.

4. Discussion

Table 3 summarises aggradation rates as measured at all sites. We have determined five contemporary bench accretion rates (31; 10; 2.3; 13, 23 mm/a) which together provide an average bench accretion rate of 16 mm/a. This value is similar to other bench accretion rates measured in northern and south eastern Australia (Hughes et al., 2010; Rustomji and Pietsch, 2007; Wasson et al., 2010). From the six estimates of contemporary aggradation rate on floodplains (0.3; 0.8; 0.2; 0.5; 0.2; 0.25 mm/a), an average of 0.37 mm/a is calculated – just 2% of that observed on the benches. The coastal plain sites likely have effectively zero contemporary aggradation rates, with the plain dominated by pedestals and scarps, remnants of a previous surface, possibly that hypothesised by Chappel et al (1982) to have existed prior to the breaching of a coastal barrier. From these data it is clear that the fastest rates of aggradation within the Normanby catchment are occurring on the within channel benches. The importance of this within the catchment wide sediment budget therefore depends on the extent of these features and the variety of aggradation rates occurring within this zone. The results obtained at the east Normanby site (Fig. 10), albeit limited though they are, allow us to address this latter question. Fig. 10b provides a plot of aggradation rate relative to the surface height above the thalweg, showing clearly that aggradation rates drop markedly, from near 1000 mm/a to 0.4 mm/a as the elevation above the thalweg increases. What is of most interest to us here, in terms of the wider significance of this result, is the gross scale of change, i.e. by how many orders of magnitude does the aggradation rate differ from the lowest bench to that surface just below the floodplain? An appreciation of this value can then be used to upscale the point data we have collected to the catchment as a whole. Although at first glance Fig 11 might be interpreted as indicating aggradation of bench surfaces varies across four orders of magnitude, we believe this would be an overestimate of the range experienced at most sites. The large range measured at this site is entirely a function of the ~1000 mm/a value measured on the point bar, a feature clearly related to bed transport and likely to be a transient feature equivalent to the similar scale, more or less linear bars of sand and gravel found throughout the catchment. We therefore consider the range encompassed by the three scroll bars (i.e. ~2 orders of magnitude) more likely to represent the range found throughout the catchment. This accords with our measurements of bench aggradation elsewhere, which show that 20 – 30 mm/a is the maximum aggradation rate for more or

less permanent features sitting relatively close to the thalweg (such as the west Normanby and Carrols Crossing benches) but which have residence times of many decades to centuries, whilst the lowest floodplain aggradation rates provide a useful minimum value.

Of note is that most bench sites are predominantly post-European in age. The West Normanby, Carols Crossing and Battle Camp benches shows evidence of 2-3m of aggradation following European Settlement, and no real evidence for upward fining as might be expected with increasing elevation above the channel. The Carols Crossing site is interesting in that it has a basal age of 1300 years, which provides some evidence for a significant increase in aggradation rates in the post-European period. A possible alternative explanation here is that the bench may have undergone incomplete stripping and redeposition, and as such it does not represent continuous deposition, and therefore precludes any interpretation of pre- and post-European aggradation rates. We would expect a gradual decrease in aggradation rates over time with an increase in surface elevation over time, as demonstrated by the ~2 orders of magnitude variation derived from the East Normanby transect (Figure 10). Using this relationship, a 1m increase in elevation from, say, 3 m to 4m above the thalweg of a 10 m deep channel, would result in a 32% decline in aggradation rate. The one bench site from which we can derive a pre-European aggradation rate (KPWN5) shows an average aggradation rate of 2.3mm/yr – which is an order of magnitude less than the average post-European rates from all other sites. Further analysis is required at this site to determine whether there is any evidence of more recent stripping episode.

Interestingly, none of the floodplain sites shows evidence of accelerated deposition following European Settlement, though it is arguable whether or not our technique is sufficiently precise to allow observation of anything less than a catastrophic increase in aggradation rate of the types seen in some settings in south eastern Australia. At the very least however, we can rule out the presence of any units of 'post settlement alluvium' of the type often observed in depositional settings in south eastern Australia.

Having observed rates of aggradation at a number of sites, we now turn to the task of estimating a total aggradation volume for in-channel benches. Cognisant of the inherent variability between sites, and therefore wary of the gains to be had from an overly complex working of our data, we have taken a parsimonious approach to estimating total aggradation for each LiDAR block and thence the catchment as a whole. Firstly we have derived a simple summed distribution for each site and multiplied this by a standard exponential function relating aggradation rate to height above thalweg (Fig. 12). The limits on this exponential function are set by observing the spread between the peak corresponding to the thalweg and the peak corresponding to the floodplain in the plots of Fig. 4, with the upper aggradation rate at all sites set to 20mm/a and the lower set to 0.2mm/a. This provides a bench area weighted average aggradation rate unique to each LiDAR block and depends on the specific distribution of surfaces between thalweg and floodplain for each site. Those channel reaches that are dominated by low lying surfaces will have higher bench area weighted average aggradation rates, while those dominated by higher surfaces, sitting closer to the floodplain will have correspondingly lower bench area

weighted average aggradation rates. Each reach specific bench area weighted average aggradation rate is then multiplied by the sum total flat area lying between the thalweg and floodplain peaks within the distribution plots of Fig.4 to give a total annual aggradation volume for each LiDAR block. This is then corrected for channel length (determined when digitising the thalweg), estimated sediment density (1.8 tonnes / m3) and average silt/clay content (26% – see PSA results in Table 3) to give an annual storage of silt/clay per stream km (Table 1). Finally, these values are used to interpolate and extrapolate annual storages of silt/clay per km in channel reaches not included in the LiDAR coverage. Where reaches have no LiDAR coverage upstream or downstream, then the average value measured across all LiDAR blocks has been applied (Fig. 13). The total annual in channel storage of fine sediment across the catchment, calculated, in the first instance, as the sum of the estimated storage in each reach is 465 ktonnes. This figure however, does not account for differences in sediment supply and presence / absence of competing depositional zones, as material is routed through the catchment. Refinements to this figure that take into consideration spatial variations in sediment supply through the catchment require the construction of a sediment budget, such as that described by Spencer et al (2012). Using detailed measurements of erosion sources throughout the Normanby catchment, in combination with a new spatially and temporally explicit catchment sediment model, they estimate an average annual input of fine sediment from all sources of 2.92 Mtonnes. Spencer et al (2012) has incorporated the results of the present study into this routing model showing that, of the 2.92 Mt / a input, 1.7 Mt (58%) is stored en route to the catchment outlet. Of this 1.7 Mt, 424 kt (25%) can be accounted for by storage on within channel benches, with the remainder stored on the upper floodplain.

Fig 13. Derived map of tonnes/silt per km stored annually within the channel.

Clearly, for channels to remain a conduit of water and sediment over the long term they cannot continue to accumulate material indefinitely. The storage of sediment within the channel could be part of a pulsed sediment discharge regime, whereby internal thresholds establish within the system that are periodically crossed, perhaps by rare cyclones, resetting to some extent the channel dimensions by broadscale in-channel bench removal and export. Alternatively Some mechanism must operate to periodically reset the system .

5. Conclusion

This study has confirmed that within channel sediment stores play an important role in the sediment budget of the Normanby catchment. 25% of all storage within the catchment occurs within the channel. Additionally, in-channel storages have ages extending from many decades to many centuries, indicating that regardless of the precise mechanism of system resetting or re-equilibrating, these sites play an important role in mediating sediment export over timescales of significance to catchment management.

Acknowledgements

References

Aitken, M.J. (1998) An introduction to optical dating. Oxford University Press, Oxford.

Dietrich, W. and Dunne, T., 1978. Sediment budget for a small catchment in mountainous terrain. Zeitschrift Fur Geomorphologie, Suppl. Bnd. 29, pp 191–206.

Dunne, T. and Leopold, L.B., 1978. Water in Environmental Planning. W.H. Freeman, San Francisco.

Dietrich, W. and Dunne, T., 1978. Sediment budget for a small catchment in mountainous terrain. Zeitschrift F Geomorphologie, Suppl. Bnd. 29, pp 191–206.

Dunne, T. and Leopold, L.B., 1978. Water in Environmental Planning. W.H. Freeman, San Francisco.

Finlayson, B.L., McMahon, T.A., 1988. Australia vs. the world: a comparative analysis of stream–flow characteristics. In: Warner, R.F. (Ed.), Fluvial Geomorphology of Australia. Academic Press, Sydney, pp. 17–40. Ch.2.

Galbraith. R. F., Laslett, G. M., 1993, Statistical models for mixed fission track ages. Radiation Measurements 21, 459–470.

Galbraith, R.F., Roberts, R.G., Laslett, G.M., Yoshida, H., Olley, J.M., 1999. Optical dating of single and multiple grains of quartz from Jinmium rock shelter, northern Australia, part 1, Experimental design and statistical models. Archaeometry 41, 339–364.

Hughes, A.O., Croke, J.C., Pietsch, T.J. and Olley, J.M., 2010. Changes in the rates of floodplain and in-channel bench accretion in response to catchment disturbance, central Queensland, Australia. Geomorphology, 114(3): 338–347.

Jacobs, Z., Duller, G.A.T., Wintle, A.G., 2006. Interpretation of single grain De distributions and calculation of De. Radiation Measurements 41, 264–277.

Jardine, T.D., Pettit, N.E., Warfe, D.M., Pusey, B.J., Ward, D.P., Douglas, M.M., Davies, P.M., Bunn, S.E. 2012. Consumer–resource coupling in wet–dry tropical rivers. Journal of Animal Ecology 81, 310–322.

Kemp, J. (2004). Flood channel morphology of a quiet river, the lachlan downstream from cowra, southeastern australia. Geomorphology, 60(1–2), 171–190.

Leslie, C., Hancock, G.J., 2008. Estimating the date corresponding to the horizon of the first detection of 137Cs and 239+240Pu in sediment cores. Journal of Environmental Radioactivity 99, 483–490

Mejdahl, V., 1979. Thermoluminescence dating: beta-dose attenuation in quartz grains. Archaeometry 21, 61–72.

Murray, A.S., Marten, R., Johnston, A., Martin, P., 1987. Analysis for naturally occurring radionuclide's at environmental concentrations by gamma spectrometry. Journal of Radio Analytical and Nuclear Chemistry 115, 263–288.

Olley, J.M., Pietsch, T. and Roberts, R.G., 2004. Optical dating of Holocene sediments from a variety of geomorphic setting using single grains of quartz. Geomorphology, 60: 337–358.

Pietsch, T.J., Olley, J.M., Nanson, G.C. (2008) Fluvial transport as a natural luminescence sensitiser of quartz. Quaternary Geochronology 3, 365–376.

Pietsch, T.J., 2009. Optically stimulated luminescence dating of young (<500 years old) sediments: Testing estimates of burial dose. Quaternary Geochronology 4, 406–422.

Prescott, J.R., Hutton, J.T., 1994. Cosmic ray contributions to dose rates for luminescence and ESR dating: large depths and long-term time variations. Radiation Measurements 23, 497–500.

Roberts, R.G., Galbraith, R.F., Yoshida, H., Laslett, G.M., Olley, J.M., 2000. Distinguishing dose populations in sediment mixtures: a test of single-grain optical dating procedures using mixtures of laboratory-dosed quartz. Radiation Measurements 32, 459–465.

Rustomji, P., Bennett, N., & Chiew, F. (2009). Flood variability east of australia's great dividing range. Journal of Hydrology, 374(3–4), 196–208.

Rustomji, P. and Pietsch, T., 2007. Alluvial sedimentation rates from southeastern Australia indicate post-European settlement landscape recovery. Geomorphology, 90(1–2): 73–90.

Stokes, S., Ingram, S., Aitken, M.J., Sirocko, F., Anderson, R., Leuschner, D., 2003. Alternative chronologies for late Quaternary (Last Interglacial e Holocene) deep-sea sediment via optical dating of silt-size quartz. Quaternary Science Reviews 22, 925–941.

Wasson, R.J. et al., 2010. Sediment sources and channel dynamics, Daly River, Northern Australia. Geomorphology, 114(3): 161–174.

TABLES

Sample	^{238}U	^{226}Ra	^{210}Pb	^{232}Th	^{40}K	D.R. (Gy/ka)	D_e (Gy)	Age
GU 2.1 Battle Camp Crossing 110 cm	25.1 ± 1.8	25.5 ± 0.4	27.2 ± 2.2	33 ± 0	476 ± 11	2.44 ± 0.18	0.23 ± 0.014	95 ± 10 a
GU 2.2 Battle Camp Crossing 320 cm	44 ± 2	43 ± 1	39 ± 3	55 ± 1	483 ± 11	2.98 ± 0.25	0.48 ± 0.02	160 ± 15 a
GU 2.3 Bizant Gully 100 cm	52 ± 3	57 ± 1	53 ± 3	74 ± 1	483 ± 11	3.55 ± 0.31	12.61 ± 0.32	3.55 ± 0.34 ka
GU 2.4 Bizant Gully 150 cm	60 ± 3	56 ± 1	52 ± 3	79 ± 1	475 ± 11	3.60 ± 0.32	12.99 ± 0.52	3.61 ± 0.37 ka
GU 2.5 Bizant Gully 200 cm	61 ± 3	67 ± 1	66 ± 3	80 ± 1	432 ± 10	3.68 ± 0.33	13.09 ± 0.40	3.56 ± 0.36 ka
GU 2.6 Bizant River 100 cm	45 ± 2	42 ± 1	36 ± 3	58 ± 1	350 ± 9	2.69 ± 0.24	2.74 ± 0.078	1.02 ± 0.10 ka
GU 2.7 Bizant River 150 cm	43 ± 2	34 ± 0	36 ± 2	58 ± 1	323 ± 7	2.58 ± 0.23	3.42 ± 0.052	1.32 ± 0.12 ka
GU 2.8 Bizant River 200 cm	45 ± 2	54 ± 1	53 ± 2	58 ± 1	266 ± 6	2.65 ± 0.24	5.88 ± 0.078	2.22 ± 0.22 ka
GU 2.9 IBA 16 Floodplain 100 cm	19.7 ± 1.0	17.4 ± 0.3	16.8 ± 1.2	21.8 ± 0.4	28.9 ± 1.3	0.89 ± 0.09	29.0 ± 0.8	32.7 ± 3.4 ka
GU 2.10 IBA 16 Floodplain 50 cm	43 ± 1	40 ± 1	35 ± 2	51 ± 1	60 ± 2	1.78 ± 0.18	4.5 ± 0.3	2.53 ± 0.31 ka
GU 2.19 Kingsplains Pit 5 100 cm	38 ± 2	38 ± 1	36 ± 2	52 ± 1	495 ± 11	2.96 ± 0.24	1.28 ± 0.05	430 ± 41 a
GU 2.20 Kingsplains Pit 5 150 cm	39 ± 2	38 ± 1	39 ± 3	54 ± 1	487 ± 11	2.99 ± 0.25	1.96 ± 0.07	660 ± 62 a
GU 2.21 Morehead R. FP 1 50 cm	44 ± 2	41 ± 1	37 ± 2	44 ± 1	205 ± 5	2.09 ± 0.19	5.88 ± 0.16	2.81 ± 0.28 ka
GU 2.22 Morehead R. FP 1 100 cm	21.9 ± 0.9	21.5 ± 0.3	20.8 ± 1.1	22.7 ± 0.3	58 ± 2	1.04 ± 0.10	5.02 ± 0.49	4.83 ± 0.66 ka
GU 2.23 Morehead R. FP 1 150 cm	18.0 ± 0.8	18.1 ± 0.2	18.4 ± 1.1	20.0 ± 0.3	37 ± 1	0.89 ± 0.08	9.02 ± 0.06	10.14 ± 1.01 ka
GU 2.24 Morehead R. FP 1 180 cm	12.1 ± 0.7	10.5 ± 0.2	11.2 ± 0.8	11.8 ± 0.2	22.2 ± 1.0	0.60 ± 0.06	18.97 ± 0.4	31.7 ± 3.2 ka
GU 2.25 Normanby R. FP 1 50 cm	38 ± 2	41 ± 1	35 ± 2	54 ± 1	346 ± 8	2.58 ± 0.22	1.49 ± 0.15	575 ± 80 a
GU 2.26 Normanby R. FP 1 100 cm	48 ± 2	49 ± 1	39 ± 3	68 ± 1	470 ± 11	3.21 ± 0.27	1.84 ± 0.25	575 ± 95 a
GU 2.27 Normanby R. FP 1 150 cm	54 ± 2	48 ± 1	44 ± 3	74 ± 1	444 ± 10	3.30 ± 0.29	no D_e	no date
GU 2.28 Normanby R. FP 1 200 cm	84 ± 3	55 ± 1	53 ± 3	71 ± 1	415 ± 9	3.41 ± 0.31	2.22 ± 0.22	645 ± 90 a
GU 2.29 Normanby R. FP 1 290 cm	45 ± 2	59 ± 1	57 ± 3	67 ± 2	386 ± 10	3.15 ± 0.28	11.73 ± 0.36	3.73 ± 0.37 ka
GU 2.30 Normanby S.VFPit1 70 cm	79 ± 3	82 ± 1	70 ± 4	134 ± 2	1078 ± 23	6.43 ± 0.53	7.0 ± 0.41	1.09 ± 0.12 ka
GU 2.31 Normanby S.VFPit1 130cm	53 ± 3	50 ± 1	46 ± 3	84 ± 1	813 ± 18	4.50 ± 0.36	13.56 ± 0.45	3.01 ± 0.28 ka
GU 2.32 NormanbyS.VFPit 1 220cm	32 ± 2	24.1 ± 0.4	28.3 ± 2.5	47 ± 1	765 ± 17	3.47 ± 0.25	10.5 ± 0.4	3.03 ± 0.27 ka
GU 2.36 West Normanby Bench 55	21.9 ± 1.6	23.3 ± 0.4	30 ± 2	31 ± 1	558 ± 13	2.68 ± 0.20	0.0455 ± 0.0179	17 ± 7 a
GU 2.37 West Normanby Bench 125	36 ± 2	34 ± 1	38 ± 2	44 ± 1	542 ± 12	2.98 ± 0.23	0.093 ± 0.025	31 ± 9 a
GU 2.38 West Normanby Bench 170	39 ± 2	36 ± 1	38 ± 2	51 ± 1	495 ± 11	2.95 ± 0.24	0.195 ± 0.0359	66 ± 13 a
GU 2.39 West Normanby Bench 220	42 ± 2	40 ± 1	41 ± 3	53 ± 1	492 ± 11	3.02 ± 0.25	0.174 ± 0.022	58 ± 9 a
GU 2.40 East Normanby x-sec 1-200	32 ± 2	29.8 ± 0.5	36 ± 2	40 ± 1	535 ± 12	2.83 ± 0.22	15.5 ± 0.6	5.48 ± 0.50 ka
GU 2.41 East Normanby x-sec 2-70	34 ± 2	32 ± 1	29.5 ± 2.3	41 ± 1	529 ± 13	2.78 ± 0.21	2.89 ± 0.07	1.04 ± 0.09 ka
GU 2.42 East Normanby x-sec 2-170	31 ± 2	32 ± 0	36 ± 2	38 ± 1	580 ± 12	2.94 ± 0.22	5.25 ± 0.25	1.79 ± 0.17 ka
GU 2.43 East Normanby x-sec 3-60	28.8 ± 1.6	25.7 ± 0.4	22.9 ± 1.8	31 ± 0	459 ± 10	2.34 ± 0.18	0.235 ± 0.095	100 ± 40 a

GU 2.44 East Normanby x-sec 3-130	28.3 ± 1.4	26.3 ± 0.4	24.9 ± 1.7	32 ± 1	484 ± 10	2.43 ± 0.18	0.75 ± 0.074	310 ± 40 a
GU 2.45 East Normanby x-sec 3-190	29.3 ± 1.7	28.5 ± 0.4	28.2 ± 2.1	36 ± 1	487 ± 11	2.54 ± 0.20	0.83 ± 0.03	330 ± 30 a
GU 2.46 East Normanby x-sec 3-310	37 ± 2	32 ± 0	31 ± 2	41 ± 1	480 ± 11	2.64 ± 0.21	0.91 ± 0.04	340 ± 30 a
GU 2.47 East Normanby x-sec 4-20	34 ± 2	33 ± 0	44 ± 2	39 ± 1	457 ± 10	2.76 ± 0.22	0.001 ± 0.01	0 ± 4 a
GU 2.48 East Normanby x-sec 4-120	37 ± 2	33 ± 1	33 ± 2	43 ± 1	488 ± 11	2.74 ± 0.22	0.0027 ± 0.014	1 ± 5 a
GU 2.49 NKCP1-95	56 ± 2	39 ± 1	35 ± 3	64 ± 1	478 ± 11	3.15 ± 0.27	3.35 ± 0.4	1.06 ± 0.16 ka
GU 2.50 NKCP1-185	54 ± 2	39 ± 1	36 ± 3	68 ± 1	504 ± 12	3.27 ± 0.28	3.75 ± 0.17	1.15 ± 0.12 ka
GU 2.51 NKCP1-400	38 ± 2	34 ± 1	28.9 ± 2.3	54 ± 1	397 ± 9	2.57 ± 0.22	5.18 ± 0.26	2.02 ± 0.21 ka
GU 2.52 NKCP2-117	54 ± 2	38 ± 1	27.5 ± 2.5	67 ± 1	497 ± 12	3.14 ± 0.26	3.76 ± 0.85	1.20 ± 0.29 ka
GU 2.53 NKCP3-35	66 ± 2	34 ± 1	27.3 ± 2.5	62 ± 1	476 ± 11	3.07 ± 0.26	3.49 ± 0.16	1.13 ± 0.11 ka
GU 2.54 NKCP3-165cm Below Salt	31 ± 2	28.4 ± 0.4	30.0 ± 1.8	49 ± 1	422 ± 9	2.55 ± 0.21	4.53 ± 0.39	1.78 ± 0.22 ka
GU 2.55 Kalpowar Bench 30	25.3 ± 1.3	23.2 ± 0.3	25.5 ± 1.5	34 ± 0	211 ± 5	1.73 ± 0.15	0.105 ± 0.025	61 ± 15 a
GU 2.56 Kalpowar Bench 155	16.7 ± 1.1	17.5 ± 0.3	19.3 ± 1.4	26.7 ± 0.4	104 ± 3	1.18 ± 0.10	0.23 ± 0.03	195 ± 31 a
GU 2.57 Kalpowar Bench 200	18.1 ± 1.8	16.5 ± 0.3	20.5 ± 2.3	22.2 ± 0.4	164 ± 5	1.29 ± 0.11	0.21 ± 0.04	163 ± 34 a
GU 2.58 Kalpowar Upper125	19.0 ± 1.6	16.3 ± 0.3	24.4 ± 2.2	22.0 ± 0.4	134 ± 5	1.27 ± 0.11	1.52 ± 0.12	1.20 ± 0.15 ka
GU 2.59 Kalpowar Upper 200	33 ± 3	34 ± 1	36 ± 3	50 ± 1	364 ± 10	2.52 ± 0.22	7.9 ± 0.5	3.14 ± 0.35 ka
GU 2.60 Carrols Xing Bench 70	24.5 ± 1.6	21.5 ± 0.3	21.4 ± 1.9	33 ± 1	282 ± 7	1.83 ± 0.15	0.0091 ± 0.009	5 ± 5 a
GU 2.61 Carrols Xing Bench 130	26.2 ± 1.5	22.4 ± 0.4	24.2 ± 1.9	35 ± 1	294 ± 7	1.94 ± 0.16	0.06 ± 0.01	31 ± 6 a
GU 2.62 Carrols Xing Bench 210	36 ± 2	33 ± 0	34 ± 2	50 ± 1	337 ± 8	2.43 ± 0.21	0.16 ± 0.02	66 ± 10 a
GU 2.63 Carrols Xing Bench 320	34 ± 1	29.6 ± 0.4	27.0 ± 1.5	44 ± 1	382 ± 8	2.35 ± 0.19	3.15 ± 0.25	1.34 ± 0.16 ka
GU 2.64 Carrols Upper Surface 130	35 ± 1	33 ± 0	29.9 ± 1.4	49 ± 1	448 ± 9	2.68 ± 0.22	58 ± 3.4	21.6 ± 2.2 ka

Profile	Contemporary Aggradation Rate (mm/yr)	Period represented (years to present)	% Fines
Benches			
West Normanby	31	60	23
Battle Camp crossing	10	110	28
KPWN5	2.3	650	55
Lower Kalpowar	13	200	16
Carols Crossing	23	60	50
Average	**16**		

East Normanby			
Point Bar	1000	2	38
Scroll 1	7	100	14
Scroll 2	0.7	1000	25
Scroll 3	0.4	5500	25
Coastal Floodplain			
NKCP1	0	500	95
NKCP2+3	0	570	95
Average	**0**		
Proximal Floodplains			
Kalpowar Upper Surface	1	1000	45
Bizant Gully	0–0.3	2500	85
Bizant River	0.8	2200	85
IBA16	<0.2	2500	10
NSVF1	0.5	1000	30
MRFP	0.2	4800	25
NRFP	0.25	400	90
Average	**0.37**		

FIGURES

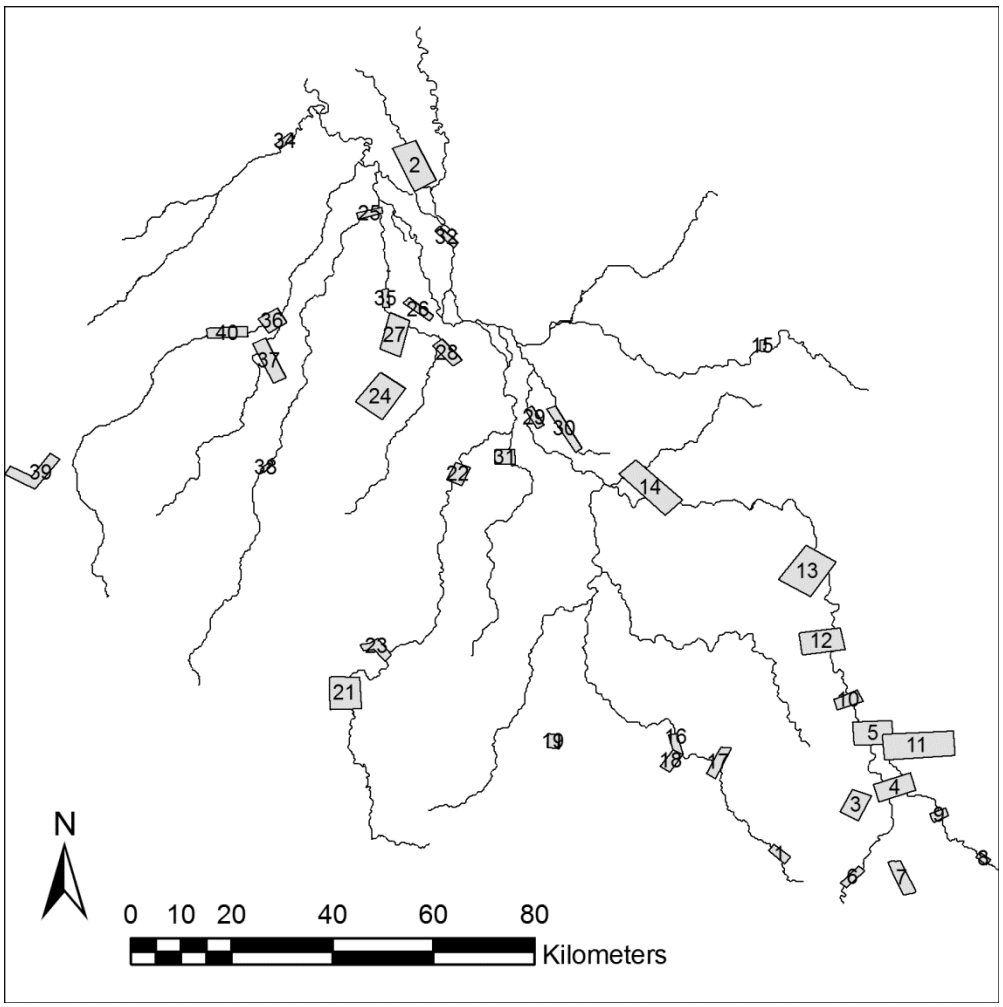

Fig.1 Map of the Normanby catchment showing major channels and location of LiDAR blocks and sampling sites.

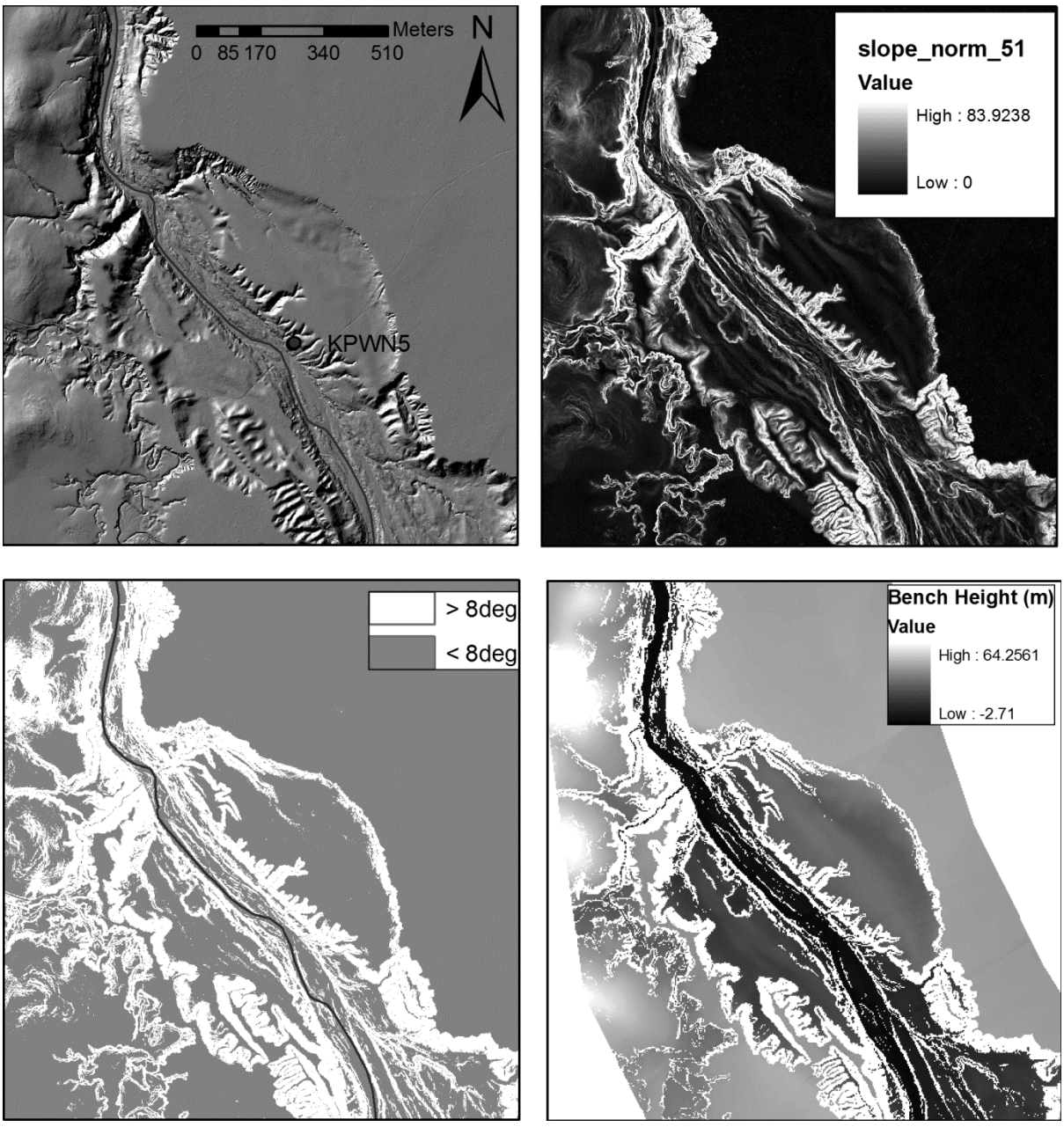

Fig. 2 Processing steps used to delineate benches using high resolution LiDAR data. Extract from LiDAR block 5 shown.

a)

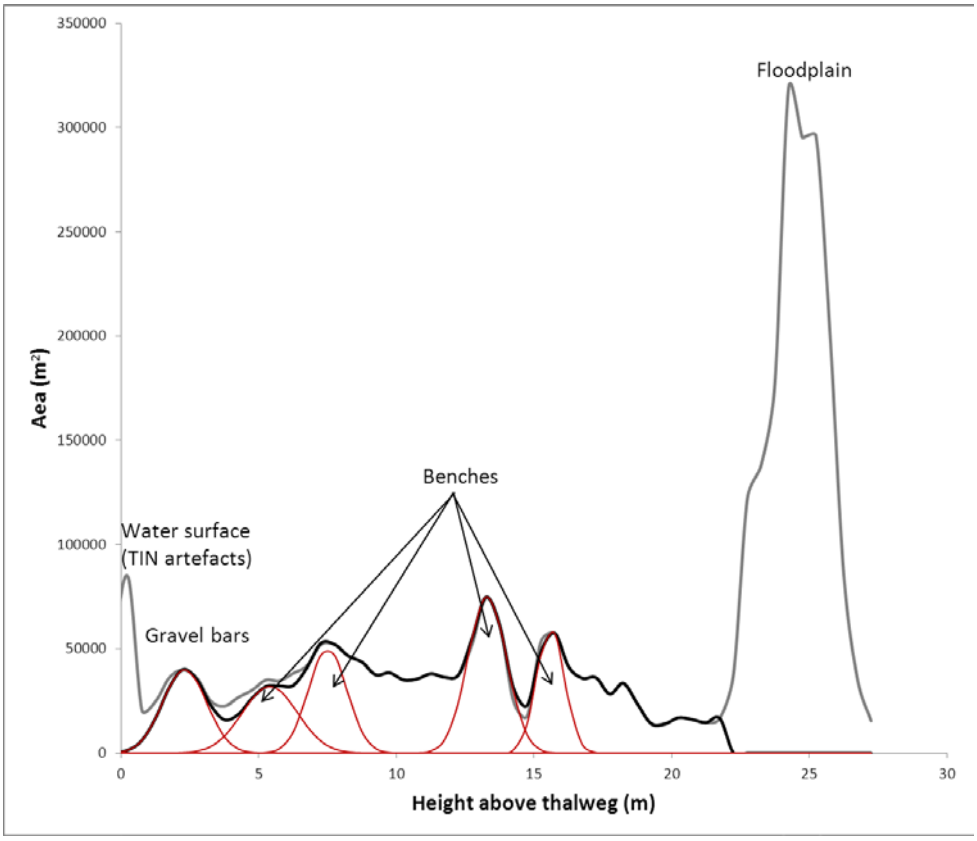
Floodplain
Benches
Water surface
(TIN artefacts)
Gravel bars
Aea (m²)
Height above thalweg (m)
350000
300000
250000
200000
150000
100000
50000
0
0
5
10
15
20
25
30

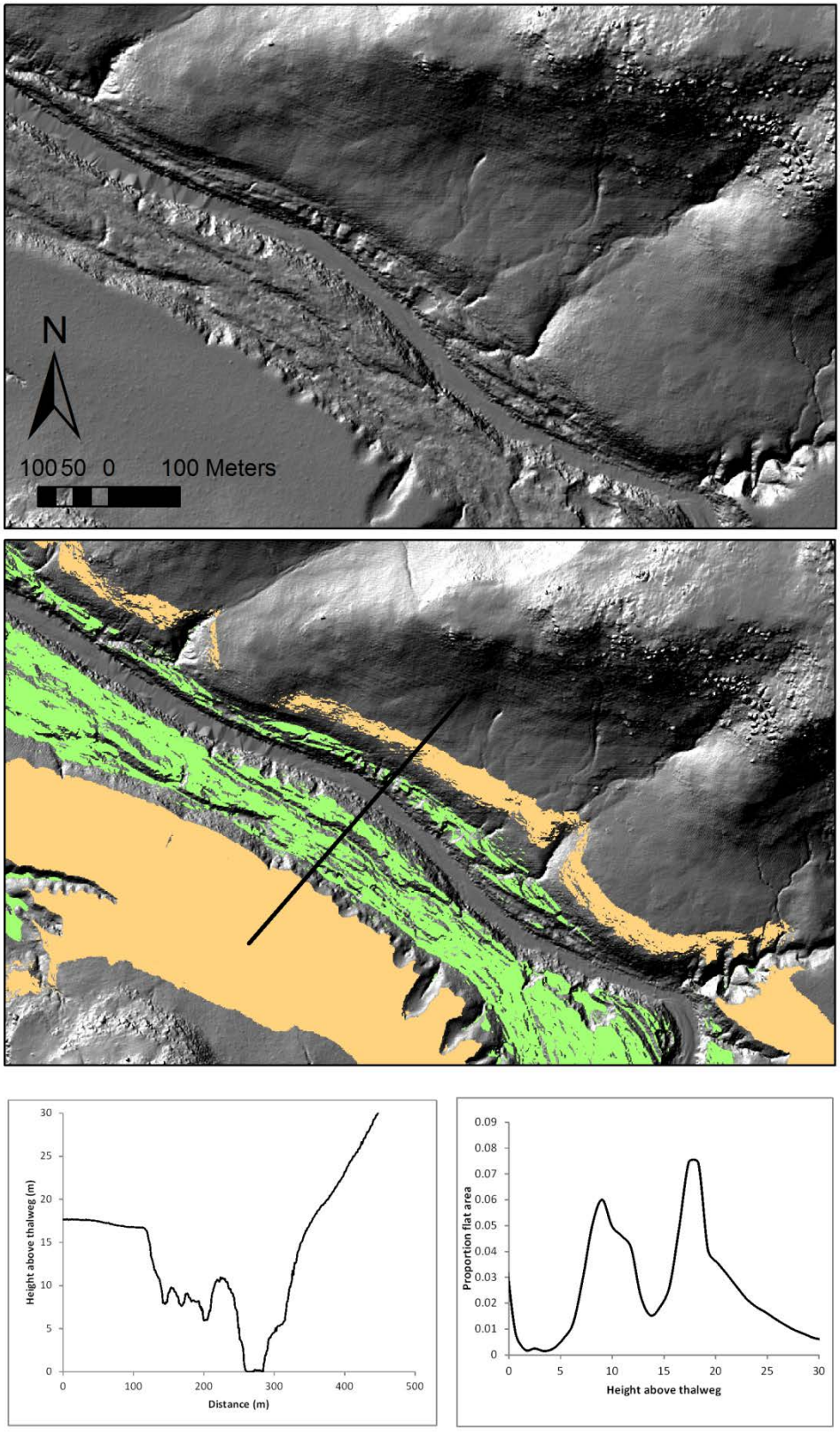

Fig.3 a) Frequency histogram for elevations above the thalweg for LiDAR block 5; b) example of fitting technique applied to Block 13

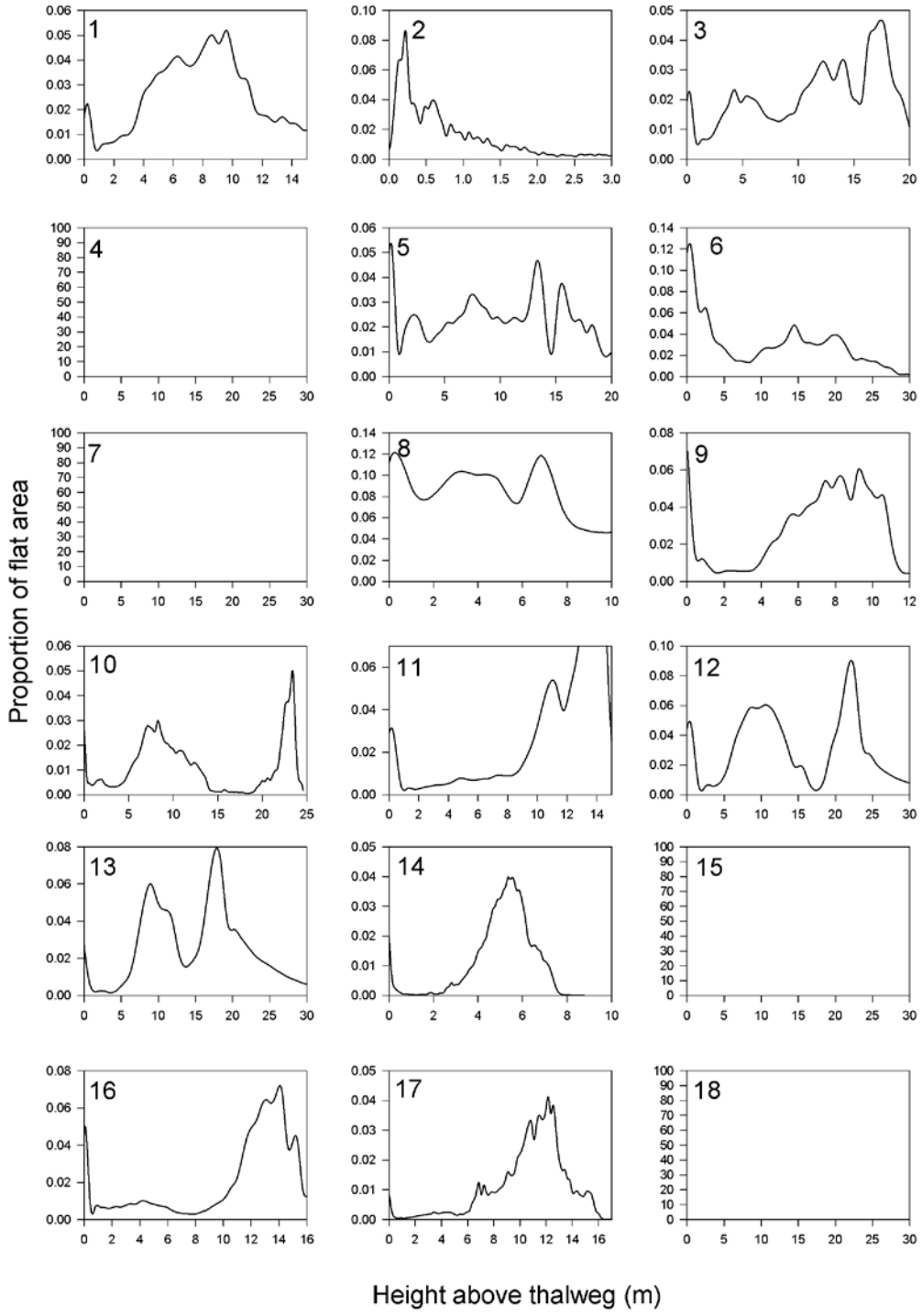
Proportion of flat area
Height above thalweg (m)
1
2
3
4
5
6
7
8
9
10
11
12
13
14
15
16
17
18

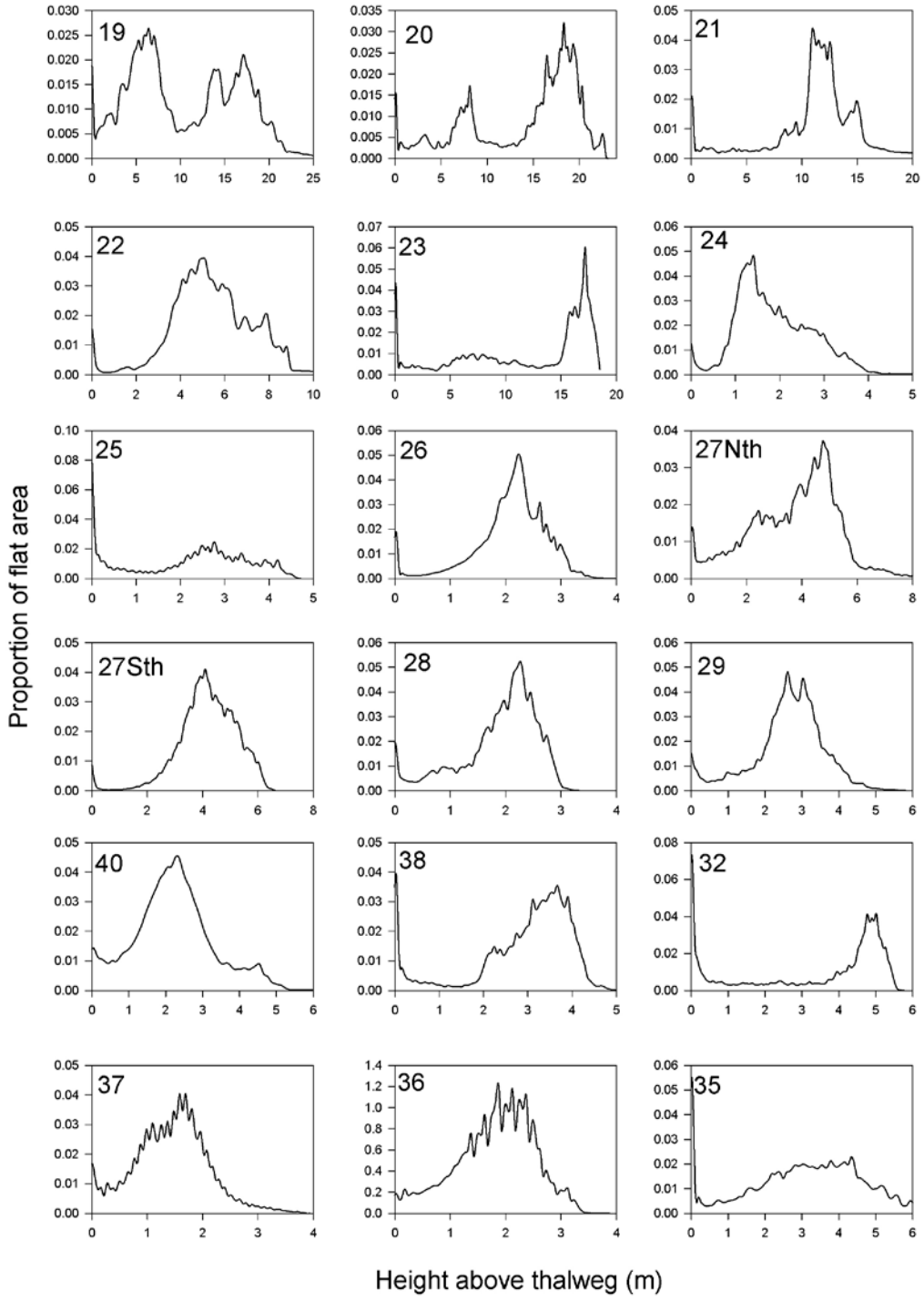

Fig. 4 Height above thalweg distributions for all LiDAR blocks. Arrow labelled 'fp' indicates floodplain in each case, whilst arrows labelled 'b' indicate benches.

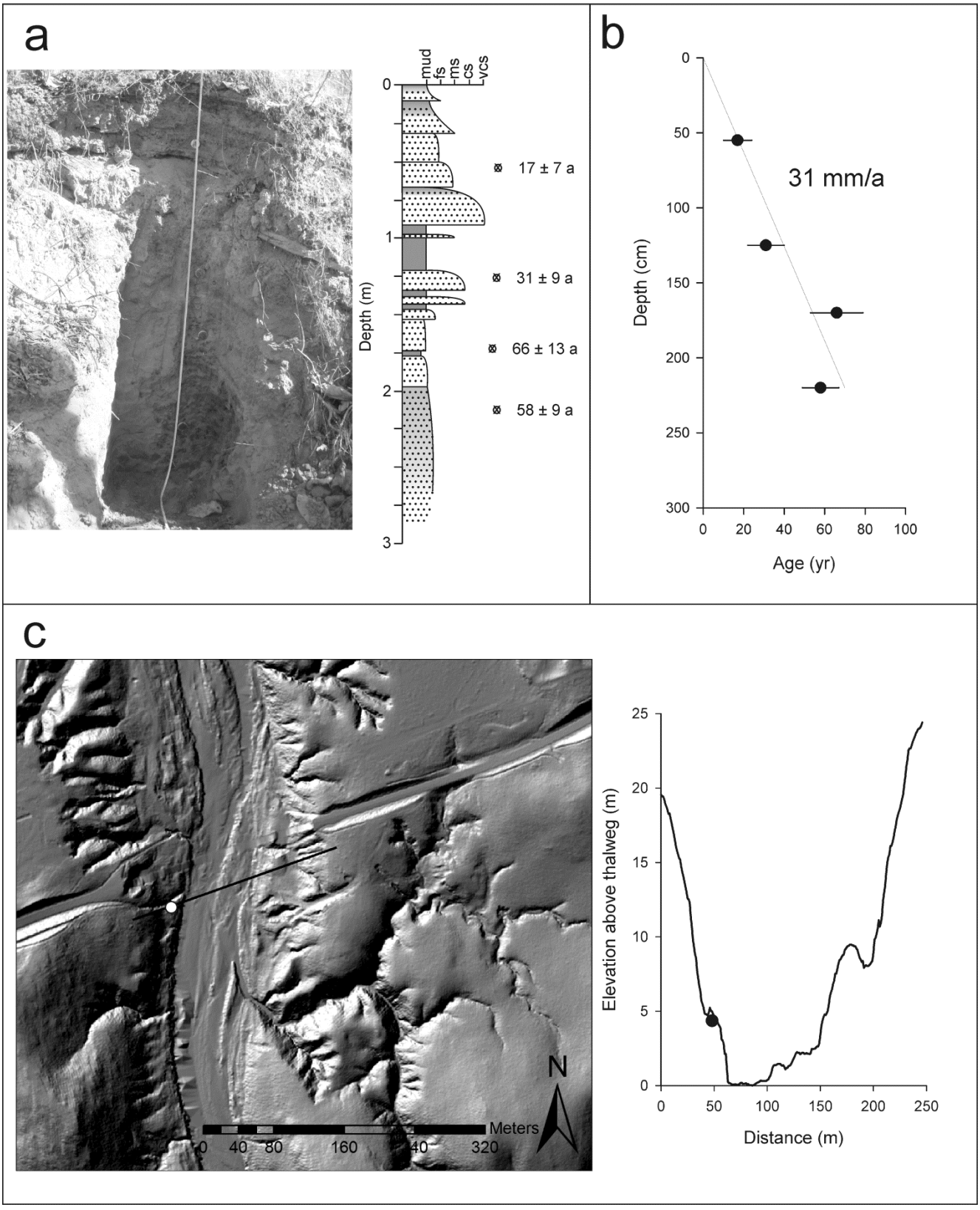

Fig. 5 a) Stratigraphy, b) OSL ages and aggradation model, and c) topography showing sampling location for the West Normanby Bench.

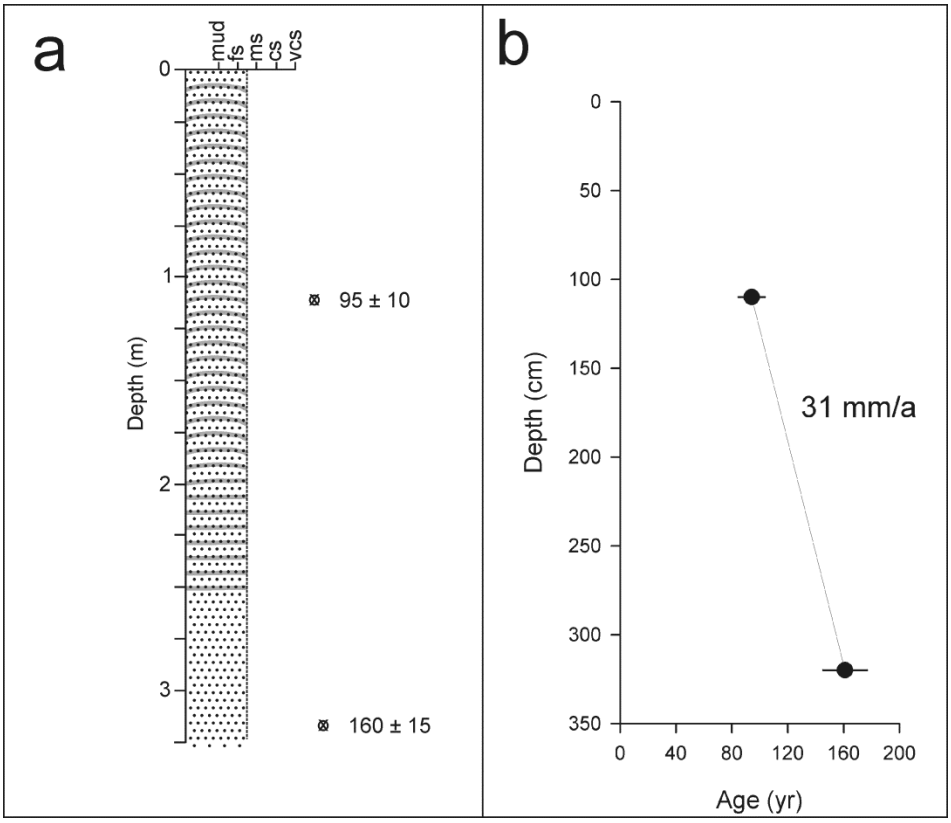

Fig. 6 a) Stratigraphy, b) OSL ages and aggradation model for the Battle Camp Crossing Bench. No cross-sectional or LiDAR data was collected for this site.

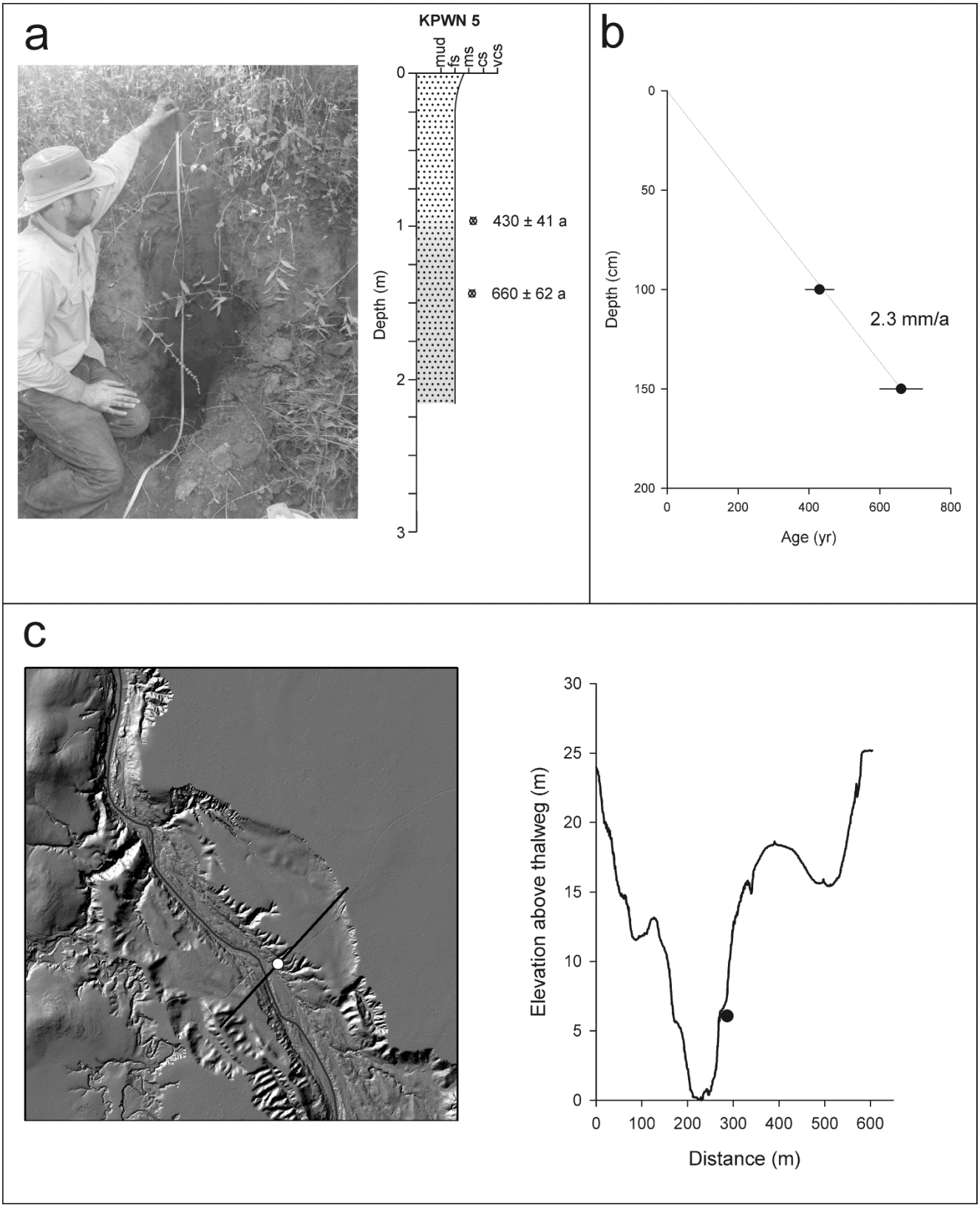

Fig. 7 Stratigraphy, OSL ages and aggradation model for the KPWN Bench

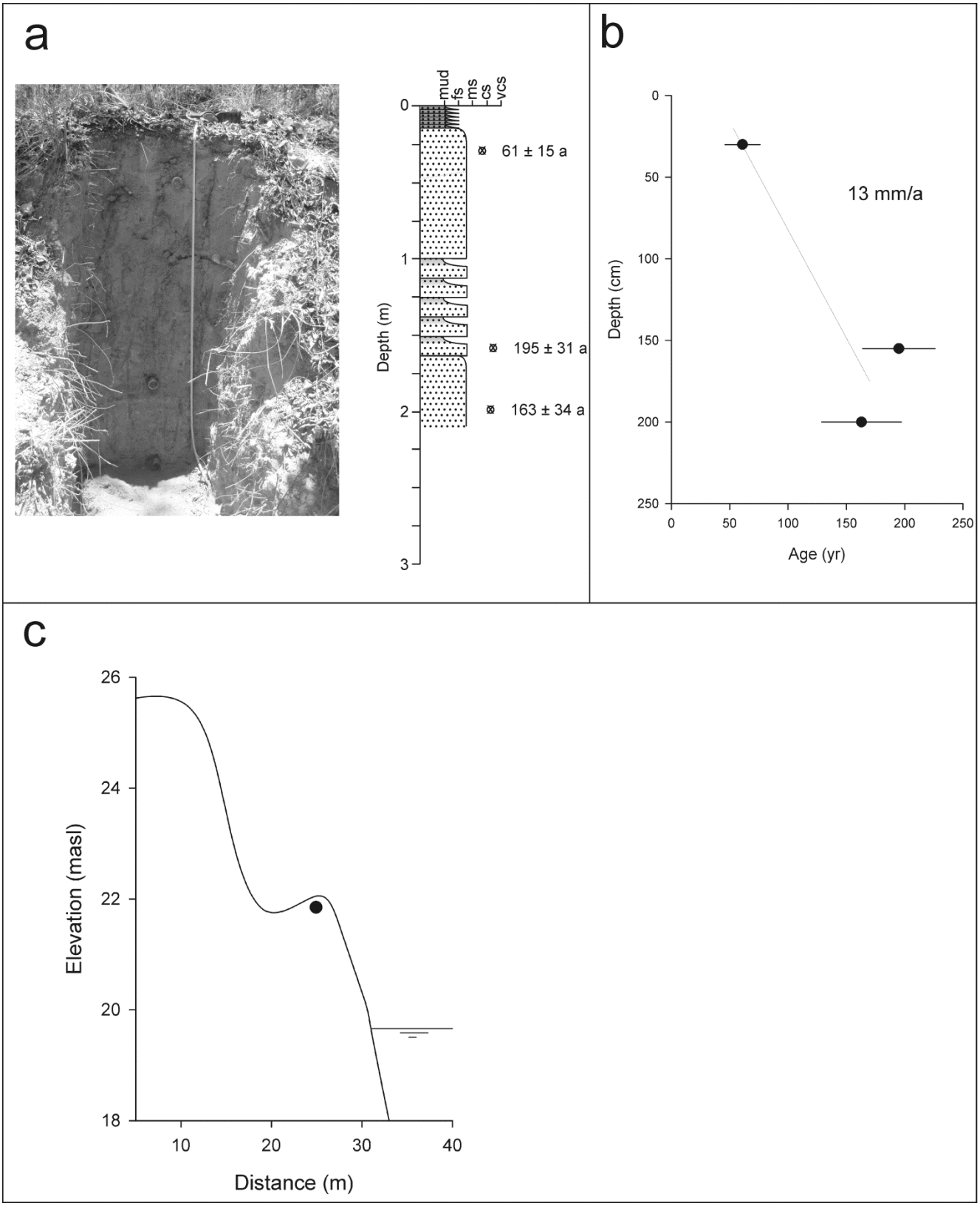

Fig.8 Stratigraphy, OSL ages and aggradation model for the Kalpowar Bench

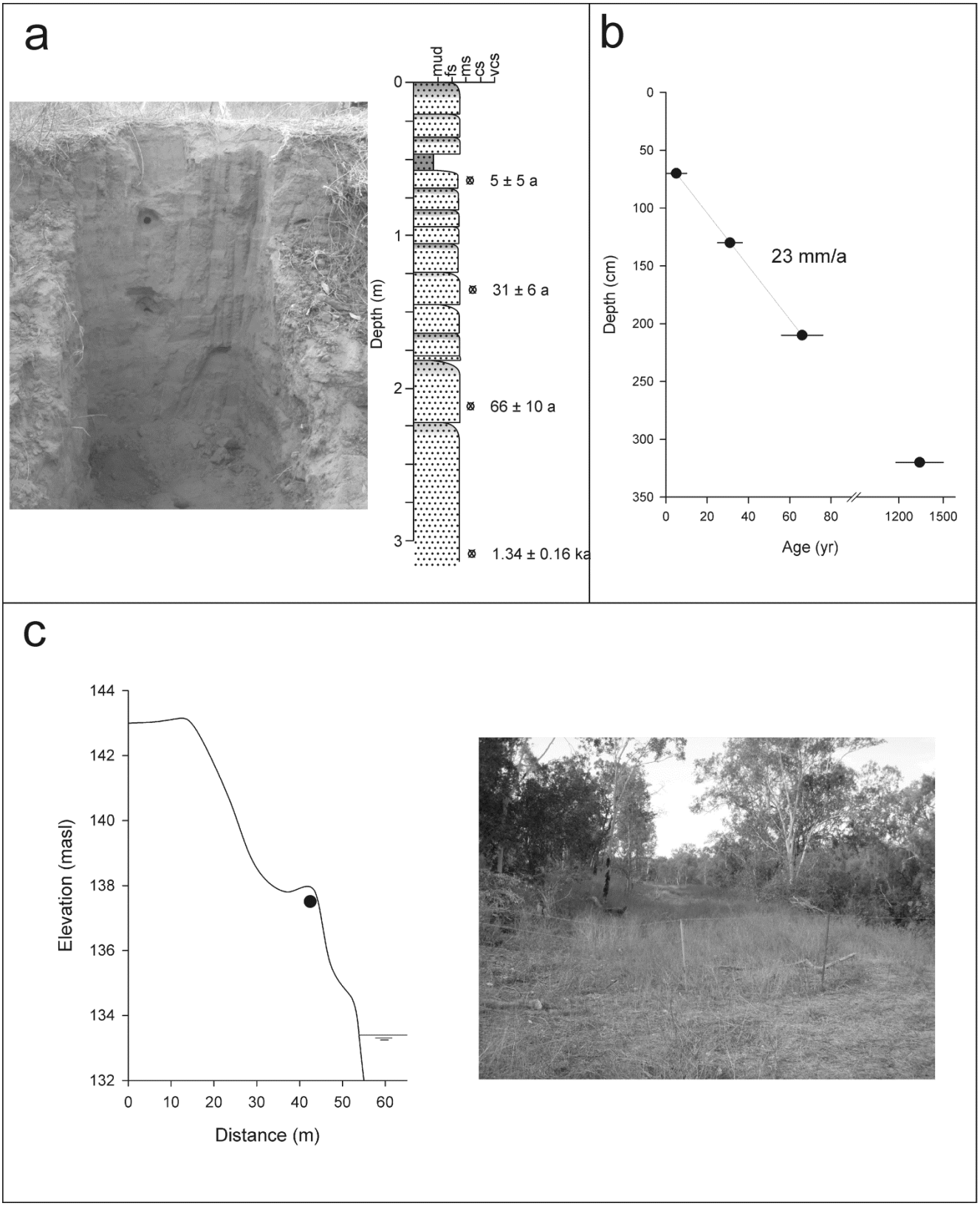

Fig.9 a) Stratigraphy, OSL ages, b) aggradation model, c) topography and photo for the Carrols Crossing Bench

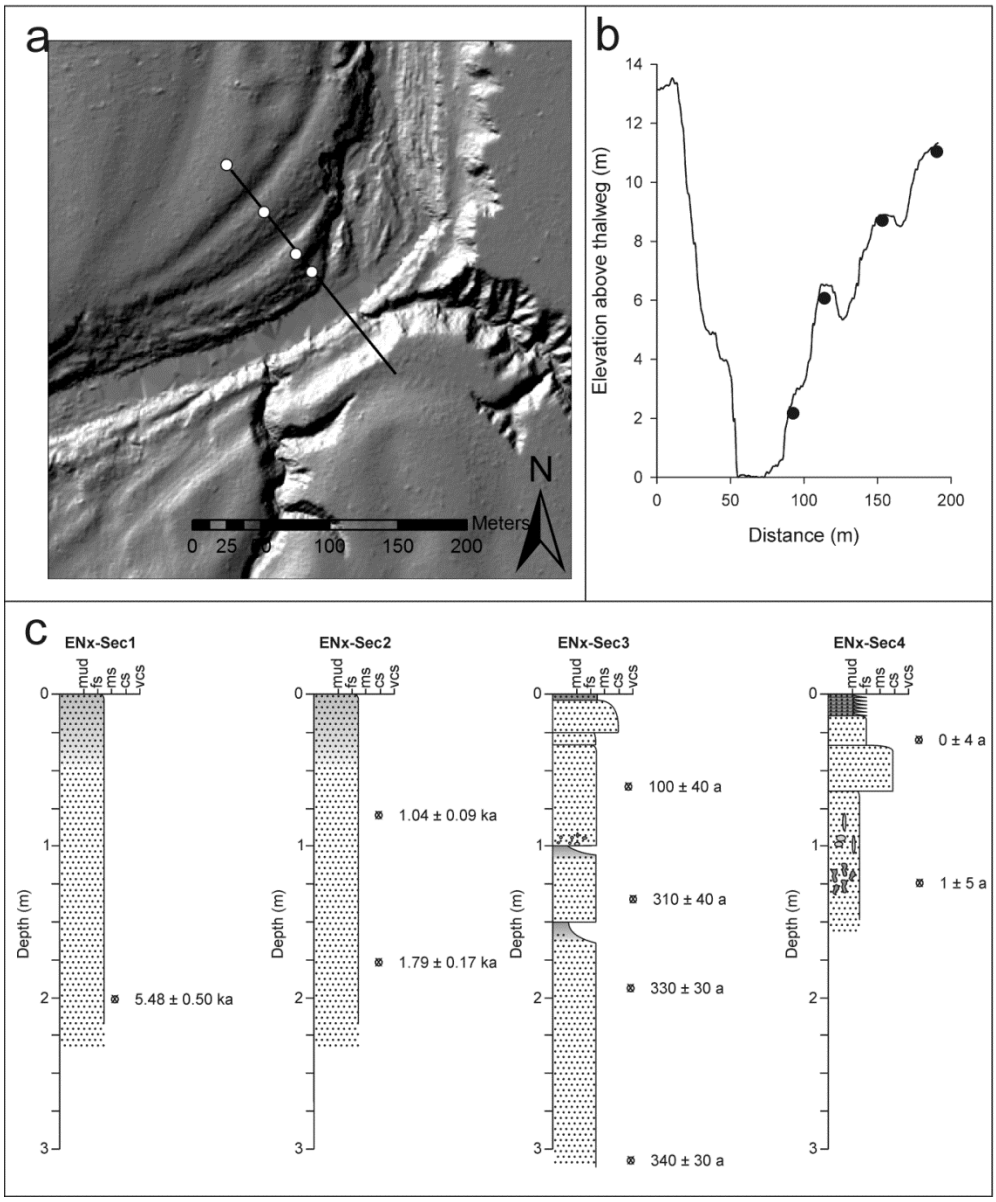
a
N
Meters
0 25 50 100 150 200
b
Elevation above thalweg (m)
Distance (m)
c
ENx-Sec1
ENx-Sec2
ENx-Sec3
ENx-Sec4
mud
fs
ms
cs
vcs
Depth (m)
5.48 ± 0.50 ka
1.04 ± 0.09 ka
1.79 ± 0.17 ka
100 ± 40 a
310 ± 40 a
330 ± 30 a
340 ± 30 a
0 ± 4 a
1 ± 5 a

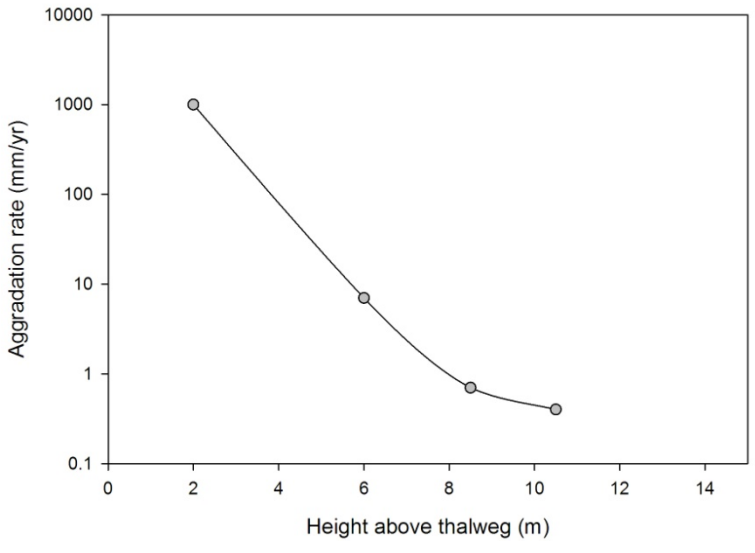
Aggradation rate (mm/yr)
Height above thalweg (m)

d

Fig. 10 Topography, stratigraphy and age structure of scroll array at East Normanby. Age model plots omitted for clarity. d) shows relationship between aggradation rate and height above thalweg.

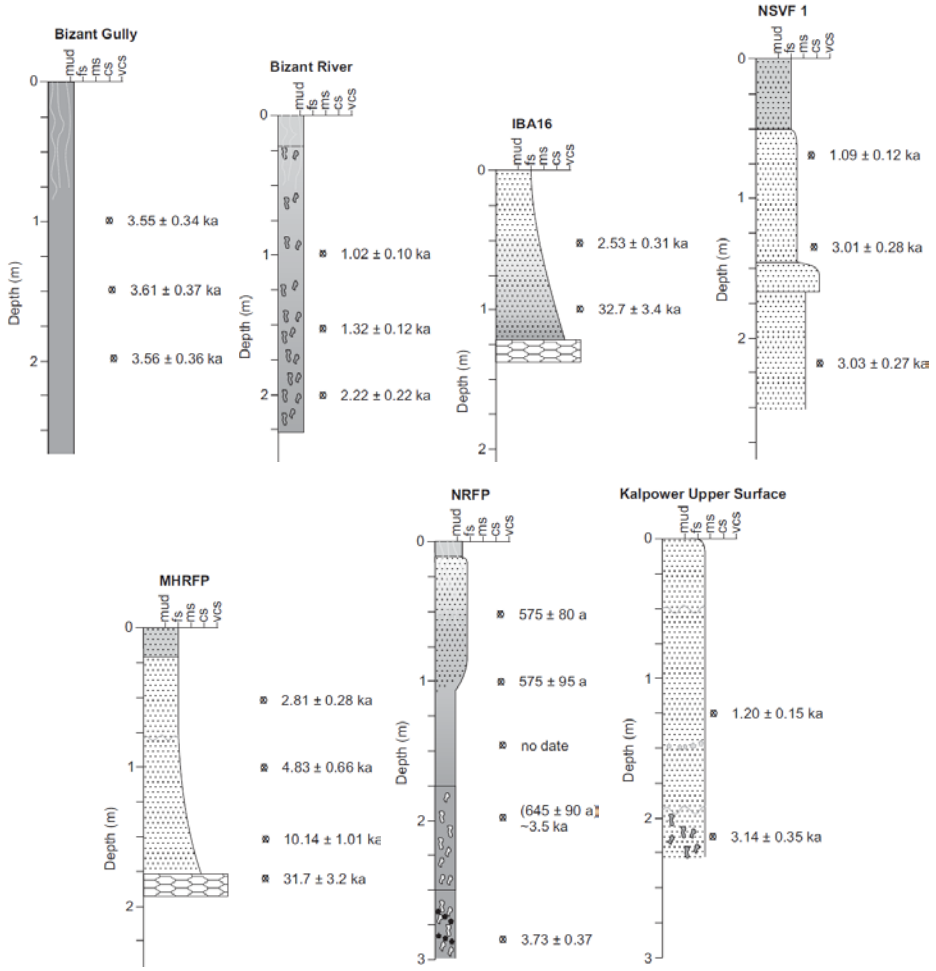

Fig. 11 Stratigraphy and age structure for the floodplain sites.

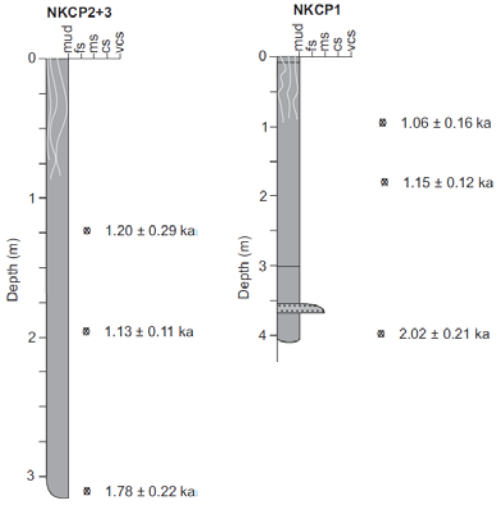

Fig 12 Stratigraphy for two sites from pedestals within coastal plain.

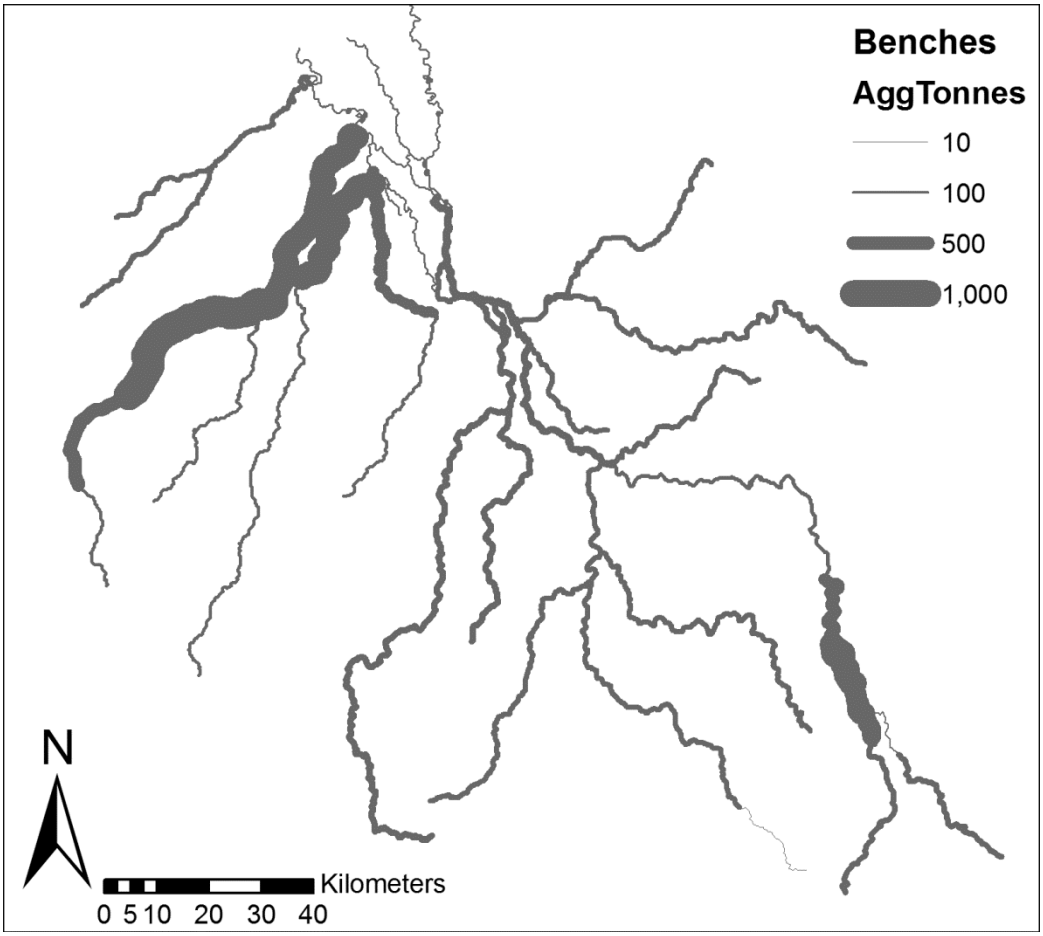

Fig 13. Derived map of tonnes/silt per km stored annually within the channel.